Check for updates

Analysis of nitro- and oxy-PAH emissions from a pilot scale silicon process with flue gas recirculation†

Kamilla Arnesen, [iD][a] Vegar Andersen,[a] Katarina Jakovljevic,[a] Ellen Katrin Enge,[b] Heiko Gaertner,[c] Thor Anders Aarhaug,[c] Kristian Etienne Einarsrud[a] and Gabriella Tranell*[a]

Silicon alloys are produced by carbothermic reduction of quartz in a submerged arc furnace. This high-temperature pyrolytic process is a source of polycyclic aromatic hydrocarbons (PAHs), which are a group of aromatic organic molecules with known mutagenic and carcinogenic properties. In this study, the emission of oxy- and nitro-PAHs from a pilot-scale Si furnace, with varying process conditions such as oxygen level, flue gas recirculation (FGR), and off-gas flow, was investigated. Analysis shows the presence of both oxy- and nitro-PAH species in all experiments, believed to be formed from radical-induced substitution reactions initiated by SiO combustion and NO_x formation. During Si production without FGR, the levels of oxy- and nitro-PAHs range between 1.1 and 4.4 μg Nm^{-3}, independent of the flue gas flow rate. With increasing FGR (0–82.5%) and decreasing oxygen level (20.7–13.3%), the concentrations of both oxy- and nitro-PAHs increase to 36.6 and 65.9 μg Nm^{-3}, respectively. When the levels of substituted PAHs increase, species such as 4-nitropyrene and 1,2-benzanthraquinone are in abundance compared to their parent PAHs. Experiments at lower flue gas flow (500 Nm^3 h^{-1} *versus* 1000 Nm^3 h^{-1}) generally produce less substituted PAHs, as well as SiO_2 particulate matter and NO_x, where the latter two parameters have a 99% correlation in this study.

Environmental significance

Polycyclic aromatic hydrocarbons (PAHs) are a group of organic molecules consisting of aromatic rings which are considered to be hazardous to human health. Some PAH molecules are proven to be carcinogenic and reduced exposure is recommended. In the silicon process, PAHs originate from pyrolysis and combustion of the carbon materials and due to the ability of PAHs to accumulate in the environment, emissions should be reduced. Substituted PAH species are not well investigated as products of industrial processes, and some argue that they have been neglected as a monitored environmental pollutant. The result of this work showed the presence of both oxy- and nitro-PAH emissions from a pilot-scale silicon furnace and levels increasing with flue gas recirculation and poorer conditions of combustion.

Introduction

Polycyclic aromatic hydrocarbons (PAHs) are a group of organic molecules consisting of two or more fused aromatic rings, with molecules classified as persistent organic pollutants, and some species are known mutagenic and carcinogenic.[1] The primary sources of PAHs in the atmosphere are incomplete combustion of organic materials such as coal, oil, petroleum, and wood.

PAHs are also emitted from natural sources such as forest fires and volcanoes, but anthropogenic activity is the main source of emission. PAH emissions from combustion are formed through two major mechanisms: PAHs produced from pyrosynthesis of carbon and hydrogen sources and emission/evaporation of existing PAHs in the original product, respectively. Both mechanisms are complex interactions affected by the fuel type, temperature, oxygen level and combustion conditions.[2]

Metallurgical grade silicon (MG-Si) is typically produced through carbothermal reduction of quartz, using a mix of coal, coke, charcoal and woodchips in a semi-closed submerged arc furnace (SAF). The carbon materials reduce the quartz to a silicon alloy by the overall reaction shown in eqn (1), where σ is the Si-yield, which gives the distribution between tapped Si and gaseous silicon monoxide (SiO) leaving the furnace.[3]

[a]*Department of Materials Science and Engineering, Norwegian University of Science and Technology (NTNU), 7034 Trondheim, Norway. E-mail: kamilla.arnesen@ntnu.no; Gabriella.tranell@ntnu.no*

[b]*Norwegian Institute of Air Research (NILU), 2007 Kjeller, Norway*

[c]*SINTEF Industry, 7034 Trondheim, Norway*

© 2024 The Author(s). Published by the Royal Society of Chemistry

Environ. Sci.: Adv., 2024, 3, 239–248 | **239**

$$SiO_2 + (1 + \sigma)C = \sigma Si + (1 - \sigma)SiO(g) + (1 + \sigma)CO(g) \quad (1)$$
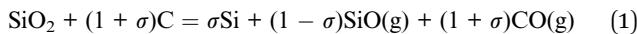
Silicon monoxide and carbon monoxide (CO) that reach the top of the furnace react with air and form silica fumes (SiO_2) and carbon dioxide (CO_2), respectively, in the furnace hood.[3]

The combustion affects the temperature at the charge surface in the furnace which can reach 700 to 1300 °C. Because the SAF is semi-closed, the under-pressure in the furnace drives the surrounding air into the furnace hood diluting the furnace off-gas, which consists mainly of air. The excess of air combined with the high temperature produces thermal NO_x through combustion, the so called Zeldovich mechanism, of nitrogen and oxygen in the air by radical formation. As described by Kamfjord,[4] the SiO and CO combustion produces high temperature hot spots at the top of the furnace charge, where also VOCs and moisture evaporate, creating conditions for fuel, prompt and thermal NO_x formation.

PAHs are emitted from the furnace, either from the top of the gas-permeable furnace charge material or through gas released during the tapping process. Typically these PAHs originate from pyrolysis, combustion of the carbon raw materials and baking of the electrodes.[5,6] Thomas and Wornat[7] described the importance of oxygen and temperature in the formation and destruction of PAHs in a high temperature reactor using catechol as a model fuel. By investigating the effect of varying oxygen levels and temperatures up to 1000 °C, oxygen is recognized to have an important role in creating free radicals that lead to increased PAH formation at $T < 850$ °C and also increased PAH destruction at $T > 850$ °C at high levels of oxygen.

In the work by Hrdina et al.,[8] parent PAH transformation through atmospheric oxidation is described, recognizing the key atmospheric oxidants of PAHs to include ozone (O_3), hydroxyl radicals (OH·), nitrogen dioxide (NO_2), and nitrate radicals ($NO_3^·$). Nitrated PAHs (nitro-PAH) and oxygenated PAHs (oxy-PAH) are two groups of substituted PAHs containing at least one nitro group (NO_2) or carbonylic oxygen attached to an aromatic ring.[9] As a result, some of the physiochemical properties change, compared to the parent PAHs, which in turn alter their environmental and toxicological effects. The International Agency for Research on Cancer (IARC) classifies 1-nitropyrene as "probably carcinogenic to humans", with PAH derivatives recognized as mutagens.[10] These electrophilic aromatic substitution reactions can occur both in gas and solid phases and produce various substituted PAHs, such as nitro- and oxy-PAH species.[11–13] Atkinson et al.[14] investigated the reactivity of naphthalene in a N_2O_5–NO_3–NO_2–air mixture under troposphere conditions and found naphthalene to form nitro-arenes by initial formation of the NO_3-PAH adduct, followed by a reaction with NO_2. The initial reaction to create a PAH adduct is seen to form both oxy and nitro-PAH species, based on the continued reaction of the adduct with available reactants, independent on the initiation of the reaction (by nitrate or hydroxyl radicals).[8,15] Oxy- and nitro-PAH compounds are also detected in research on emissions from diesel engines, where NO_x is known to be a considerable part of the exhaust. Heeb et al.[16] investigated how diesel engine filters influence PAH and nitro-PAH profiles in diesel exhaust and found the filter to promote the formation of some nitro-PAHs, enhancing the degradation of others depending on the operating conditions of the engine. Hayakawa[17] investigated the formation of nitro-PAHs compared to their parent PAHs with increasing combustion temperatures, representing diesel-engines, coal and wood burning stoves. The nitro-PAH/PAH ratio was observed to increase with temperature for compounds such as 1-nitropyrene, 6-nitrochrysene and 7-nitrobenz[a]anthracene. Oxy-PAHs have been found in emissions related to diesel exhaust, charcoal and coal production.[18] Drotikova et al.[19] measured PAHs in ambient air in Longyearbyen, Svalbard, and found coal-fired power plants to be one of the main sources of PAHs, with 9-fluorenone and 9,10-anthraquinone to be the dominating oxy-PAH species.

Flue gas recirculation (FGR), or exhaust gas recirculation, is a known method used for emission control by recycling parts of the process off-gas, e.g. in diesel engines to reduce oxygen levels, temperature and NO_x formation, and as a way to concentrate off-gas species, such as CO_2, for further processing for CO_2 capture.[20–22] The method has also been found to increase the level of hydrocarbon species (including PAHs), when temperature and oxygen concentrations reach a certain level due to reduced oxidation efficiency.[23–25] Wittgens et al.[26] investigated the possibility of including a post-combustion chamber for increased energy recovery with reduced PAH and NO_x emissions in the ferroalloy industry with positive results. Together with the PhD thesis of Andersen (2023),[27] studying flue gas recirculation (FGR) for the silicon process, and Kamfjord (2012),[4] studying NO_x formation in the silicon process, these represent a body of work forming the basis for understanding the off-gas systems and the current status for emissions of PAHs from the SAF-based Si production process.

With increased EU and global focus on industrial emissions (PM, PFAS, GHG, etc.), it will become essential for industries to better understand complex and less understood pollutants outside the regularly reported, such as in this case of PAH-16.

While the authors in previous work went in depth on an extensive list of native PAHs, to the authors knowledge this is the first study trying to determine nitro- and oxy-substituted PAH emissions from ferroalloy production as an area still to be explored. The focus for the current work was therefore to determine if, and potentially how much substituted PAHs was formed, evaluate and compare these concentration levels in the off-gas from a pilot scale silicon furnace with and without flue gas recirculation.

Experimental methodology

Pilot furnace

A pilot scale one-phase submerged arc furnace was used for silicon production with flue gas recirculation over a 3 day period with continuous operations. More details regarding the experiment can be found in the work of Andersen et al.[27–29] The furnace and off-gas system is illustrated in Fig. S2.† The off-gas composition was analyzed during the experiment using different techniques, both on the furnace outlet and inlet. Gas

composition (*e.g.* O_2, CO_2, NO_x, CO) and PM were analyzed using an Agilent 490-PRO Micro-GC, LaserGas II and LaserDust instruments (NEO monitors).

A mix of coal, coke, charcoal, woodchips and quartz made up the raw material, which were supplied by an industrial partner. The materials were used as received, except for the woodchips, which were dried at 100 °C for 24 h. Carbon raw material specifications are found in Table S3.†

PAH sampling procedure

A sample collection system for PAHs was developed by adapting a standard set-up following isokinetic sampling principles (based on ISO 11338-1:2003) to investigate PAH composition in the gas and particle phase from the pilot furnace. More details regarding the sampling method are described elsewhere.[30] The sampling set-up used glass fiber filters (22 Ø, Munktell/ Ahlstrom, Sweden) and XAD-2 (Supelpak-2, Merck Life Science AS, Germany) absorbent with a rotary vane pump (Paul Gothe GmbH, Germany) for sample extraction from the off-gas duct. All samples were protected against UV radiation by layers of aluminum foil and stored at 4 °C in a dark location prior to analysis at the Norwegian Institute of Air Research (NILU, Kjeller, Norway).

PAH analysis methodology

The analytical procedure follows the requirements of NILU's accreditation, according to NS-EN ISO/IEC 17025. Internal standards containing deuterated PAH congeners were added to all samples prior to extraction. The standards are listed in Table S4.† XAD-2 and filter samples were Soxhlet extracted for 8 h in acetone/hexane (1 : 1), concentrated followed by cleanup using silica gel deactivated with 8% water (adsorption chromatography). After concentration, recovery standards were added. The identification and quantification of a set of nitro- and oxy-PAH analyses were performed by the gas chromatography quadrupole time-of-flight (GC-qToF) method in Electron Capture Negative Ion (ECNI) mode. The list of PAH components is shown in Table 1.

Results and discussion

Each sampling period started within a new experimental cycle for the pilot furnace, after stable process conditions were reached. A cycle from feeding raw materials to charge material collapse and metal tapping lasted about 1.5 hours. Near the end of the cycle was often marked with a blowout in the furnace, which caused the furnace conditions to change, and marked the end of a stable period. A more detailed description of variations within the experiments can be found in the work of Andersen *et al.*[28]

On average, 0.30 Nm^3 off-gas was sampled per hour of silicon production. Results from 9 different experiments, out of 27 runs, will be presented in this work, which include a total of 27 samples where the FGR levels vary from 0 to 75.0% for experiments at a 500 $Nm^3 h^{-1}$ off-gas flow rate and from 0 to 82.5% for experiments at 1000 $Nm^3 h^{-1}$. An overview of the total concentration of PAH-42, oxy- and nitro-PAHs from experiments at varying FGR for 1000 and 500 $Nm^3 h^{-1}$ is presented in Fig. 1, and the results for all oxy- and nitro-compounds can be found in Table S1 in the ESI.†

The concentrations are a sum of 8 nitro-species with 3 and 4 rings, 6 oxy-species with 3 to 5 rings, and PAH-42, which represent an extended EPA-16 list that also includes heterocyclic and alkylated PAHs.

Overall, an increase in PAH concentration was observed when comparing the Si production with and without FGR for both the 1000 and 500 $Nm^3 h^{-1}$ flow rates. Higher PAH concentrations were generally observed for the 1000 $Nm^3 h^{-1}$ experiments as further elaborated by Arnesen *et al.*,[30] where the increased temperature and residence time at low flow are believed to result in better conditions for combustion. An important note is the number of species being analyzed, which represent the different categories, and analyzing 42 species would expect to result in a higher concentration than the 14 substituted PAHs.

Table 1 List of nitro- and oxy-PAH components analyzed in the FGR off-gas samples

| Compound	MW^a [g mol^{-1}]	# of rings	IARC classification^b
9-Nitroanthracene	223.2	3	Group 3
2 + 3-Nitrofluoranthene	247.3	4	Group 3
1-Nitropyrene	247.3	4	Group 2A
4-Nitropyrene	247.3	4	Group 2B
3-Nitrobenzanthrone	275.3	4	Group 2B
7-Nitrobenz[*a*]anthracene	273.3	4	Group 3
1,3-Dinitropyrene	292.2	4	Group 2B
1,6-Dinitropyrene	292.2	4	Group 2B
9-Fluorenone	180.2	3	—
9,10-Anthraquinone	208.2	3	—
2-Methyl-9,10-anthraquinone	222.2	3	—
6*H*-Benz[*de*]anthracen-6-one	230.3	4	—
1,2-Benzanthraquinone	258.3	4	—
6*H*-Benzo[*cd*]pyren-6-one	254.3	5	—

^{a} PAH MW.[31] ^{b} PAH IARC status.[10]
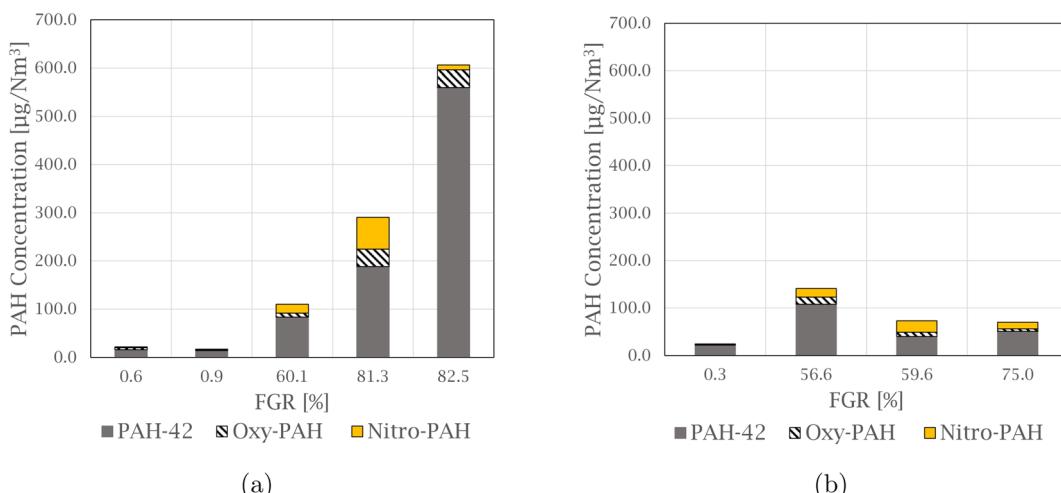
Fig. 1 Graphs showing the total PAH-42, oxy- and nitro-PAH concentrations in the off-gas at varying FGR levels for experiments at (a) 1000 Nm^3 h^{-1} and (b) 500 Nm^3 h^{-1}.
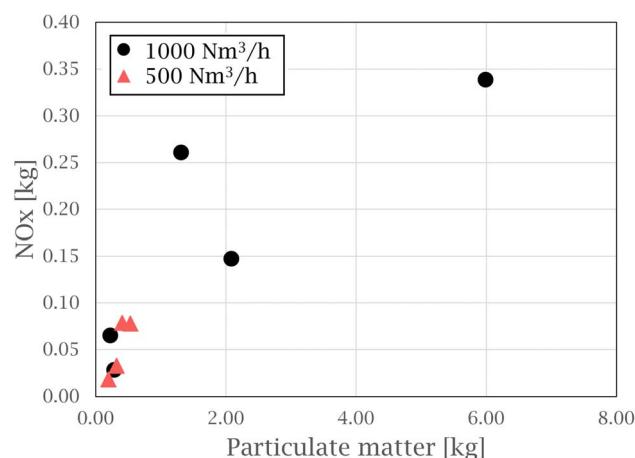
Fig. 2 Graph showing the variation in particulate matter and NO$_x$ produced during Si production, for experiments at both 1000 Nm^3 h^{-1} and 500 Nm^3 h^{-1}.

Dust and NO$_x$ production

The total amount of particulate matter (PM) and NO$_x$ was measured during the experiments, and the variations are presented in Fig. 2. NO$_x$ is the sum of NO and NO$_2$, where NO$_2$ on average makes up $13.7 \pm 2.0\%$ of the total amount. A correlation was found between PM and NO$_x$ at 99%. This correlation is also observed in experimental work performed by Kamfjord,[4] where exothermic SiO combustion to particulate silica fumes at the furnace charge surface creates local areas with high temperature, and thermal NO$_x$ can form. The level of both dust and NO$_x$ observed in the pilot experiments decreases for experiments at a lower flow, 500 Nm^3 h^{-1}, with amounts below 1.00 kg PM and 0.10 kg NO$_x$. Less ambient air is needed to dilute the off-gas at low flow, and the lower amount of oxygen available for SiO combustion can therefore be a reason for the decreased NO$_x$ levels.

Emission of nitro-PAHs during Si production

The level of measured nitro-PAHs in the pilot campaign ranges between 1.4 and 65.9 μg Nm^{-3}. Under conditions for Si production without FGR, the level of nitro-PAHs is between 1 and 2 μg Nm^{-3}. An overview of the total nitro-PAH concentrations and conditions for experiments at 1000 and 500 Nm^3 h^{-1} together with the average measured values for the experiments, flow, FGR level, oxygen level and temperatures, is presented in Table 2.

Table 2 Nitro-PAH concentrations, measured gas flow, recirculation ratio and oxygen averages from PAH sampling in the FGR Pilot campaign, sorted by flow and decreasing oxygen levels

Sample nr	Flow [Nm^3 h^{-1}]	FGR [%]	Oxygen [vol%]	Flue gas temperature [°C]	Nitro-PAH [μg Nm^{-3}]
1	965	0.6	20.7	208	1.353
8	914	0.9	20.7	249	1.869
5	935	60.1	17.6	238	18.468
4	865	81.3	15.5	232	65.867
13	919	82.5	13.3	237	9.807
9	566	0.3	20.4	268	1.678
3	440	56.6	17.9	275	18.219
7	497	59.6	17.3	293	24.010
6	425	75.0	16.4	275	14.001
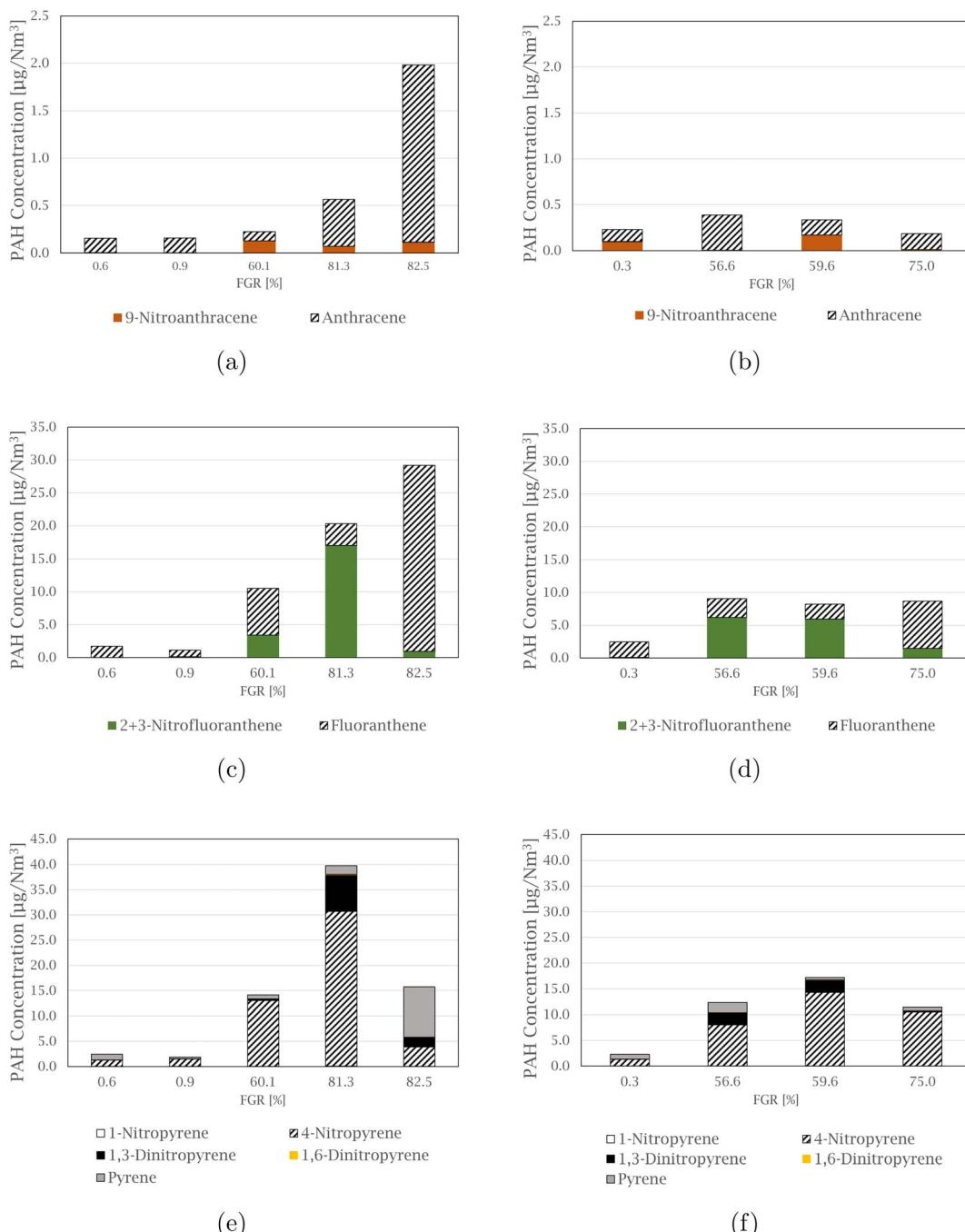
Fig. 3 Graphs showing the distribution of nitro-PAHs and the corresponding parent PAHs for experiments at 1000 Nm^3 h^{-1} (left) and 500 Nm^3 h^{-1} (right), (a and b): anthracene species, (c and d): fluoranthene species, and (e and f): pyrene species.

With some variation a general trend is observed. When combustion conditions change, the level of nitro-PAHs increases up to 65.9 μg Nm^{-3}, with lower available oxygen, which indicates that higher flue gas recirculation rates that lead to lower oxygen levels in the furnace atmosphere can be a substantial driving force for the generation of nitro-PAHs. Some variation is present between the two flow rates (500 and 1000 Nm^3 h^{-1}), where the concentration reaches higher levels for the increased flow rate. On average, 96.8% of the measured

nitro-PAH species were found in the filter samples. As expected, these species are present as a condensed phase based on molecular weight and volatility, combined with the average flue gas temperature.

The compound 4-nitropyrene is the most abundant nitro-PAH species of those quantified in every sample, accounting for 39.5 to 91.5% of the total measured nitro-PAH concentration. The second most abundant species is the combined 2 and 3-nitrofluoranthene, with levels up to 34.0% of the total

© 2024 The Author(s). Published by the Royal Society of Chemistry

Environ. Sci.: Adv., 2024, **3**, 239–248 | **243**
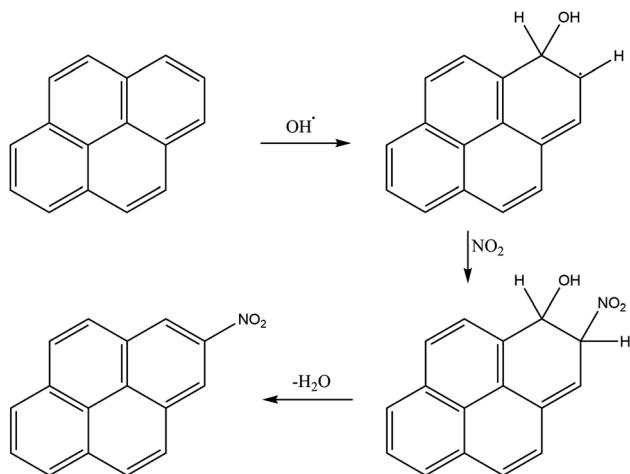
Fig. 4 An example of a nitration mechanism of pyrene with OH[•] initiating the substitution reaction.

concentration in the samples. Fig. 3 shows comparisons between the concentration of nitro-PAH species with their parent PAHs at different FGR levels (concentrations of the parent PAHs can be found in the ESI† of Arnesen et al.[30]). The anthracene species are shown in Fig. 3(a) and (b), where the parent species is in abundance for most of the experiments, with the exception of experiments at 59.6 and 60.1% FGR, where the distribution is approximately equal. For fluoranthene, in Fig. 3(c) and (d), more 2 + 3-nitrofluoranthene (separation of 2- and 3-nitrofluoranthene was not achieved with the current analysis technique) than its parent is detected in three of the nine experiments. The opposite is the case for pyrene species in Fig. 3(e) and (f), where regular pyrene is only dominating in one experiment at 82.5% FGR. Overall, the dominating pyrene species are 4-nitropyrene, followed by 1,3-dinitropyrene, which in some cases exhibit the same concentration levels as pyrene.

Even though the level of NO_x and the concentration of nitro-PAHs did not show a direct correlation with the level of flue gas recirculation in this study (5% correlation), it becomes clear that the formation of PAH species in a pyrolytic system such as the Si furnace is a balance between oxidative combustion, depending on temperature and oxygen, and other competing reactions.

Nitrogen oxides must be present for nitro-PAHs to form and NO_x forming reactions are a source of radicals and atmospheric oxidative reactions. Hrdina et al.[8] described the necessity of radicals and radical-initiated reactions to create oxidants such as NO_3^- and OH[•], which function as activators of the substitution reaction. Katritzky et al.[11] described the nature of an aromatic substitution reaction, where the initial reaction step produces a temporary positively charged arenium ion. The initial reaction to form the arenium ion is typically the rate-limiting step, which will react further with electron rich molecules. In the case of this study, oxygen or NO_2 is expected to react and form the final oxy- or nitro-PAH molecule. An example of how nitration of pyrene could occur is presented in Fig. 4.

The mechanism of the substitution reaction and preferential isomeric formation is often used to characterize PAH emissions. From studies examining nitro-PAH emissions from diesel vehicles (Hu et al.)[32] and substituted PAHs in pollution at rural and urban locations in France (Albinet et al.),[12] the isomer of 1-nitropyrene is observed and viewed as an favored isomeric pyrene specie. Atkinson et al.[14] investigated the kinetics of nitro-PAH formation and found 1- and 2-nitropyrene to be favored over 4-nitropyrene in OH radical-initiated reactions with pyrene under ambient conditions. They also determined the rate constants for gas-phase reactions in N_2O_5–NO_3–NO_2–air, and found both 2- and 4-nitropyrene to be a product of the NO_3 radical-initiated reaction. 2-Nitropyrene was found to be dependent on the NO_2 concentration, but no such connection was discovered for 4-nitropyrene. In this current study, 4-nitropyrene was the abundant pyrene species in all samples, and 4-nitropyrene is thus most likely a product of the gas-phase NO_3 radical-initiated reaction directly in the furnace and a result of a primary emission source.

Emission of oxy-PAHs during Si production

The level of oxy-PAHs measured in the pilot campaign ranges between 1.1 and 36.6 µg Nm^{-3}. On average 94.4% of all the species were found in the filter samples. This is slightly lower than for nitro-PAHs and is mainly caused by the oxy-PAHs with lower molecular weight (9-fluorenone and 9,10-anthraquinone) passing through the filter. Using bag house filters to clean dust and condensed PAH species from the off-gas is a widely used technique. Off-gas temperature is an important control

Table 3 Total oxy-PAH concentrations, measured gas flow, recirculation ratio and oxygen averages from PAH sampling in the FGR pilot campaign, sorted by flow and decreasing oxygen levels

| Sample nr	Flow [Nm³ h⁻¹]	FGR [%]	Oxygen [vol%]	Flue gas temperature [°C]	Oxy-PAH [µg Nm⁻³]
1	965	0.6	20.7	208	4.389
8	914	0.9	20.7	249	1.131
5	935	60.1	17.6	238	8.026
4	865	81.3	15.5	232	35.928
13	919	82.5	13.3	237	36.647
9	566	0.3	20.4	268	1.228
3	440	56.6	17.9	275	15.280
7	497	59.6	17.3	293	9.297
6	425	75.0	16.4	275	5.620
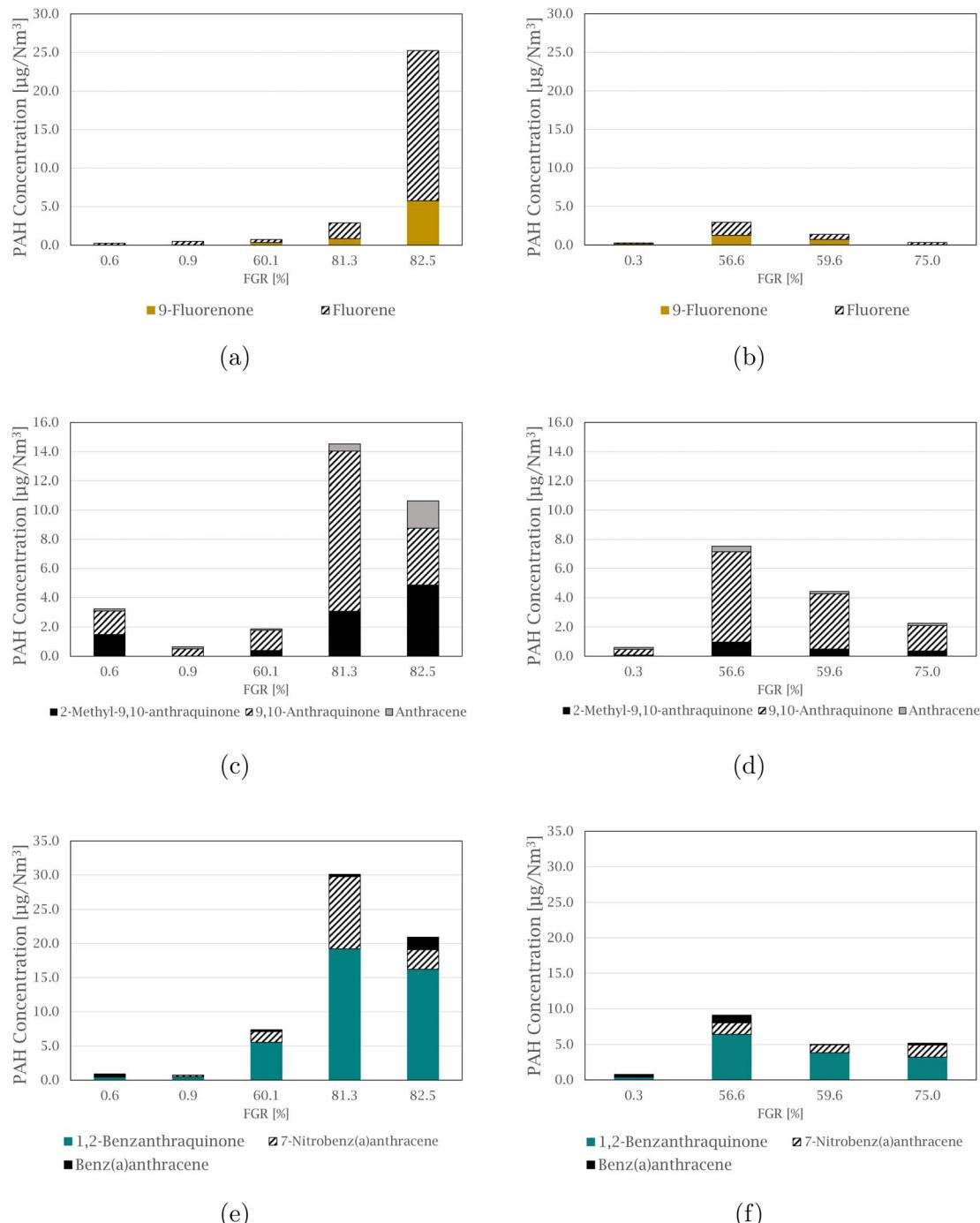
Fig. 5 Graphs showing the distribution of oxy–PAHs and the corresponding parent PAHs for experiments at 1000 Nm^3 h^{-1} (left) and 500 Nm^3 h^{-1} (right), (a and b): fluorene species, (c and d): anthracene species, and (e and f): benz(a)anthracene species.

parameter to protect the filter-bag material from degradation and ensure efficient removal of particulate matter. The total concentration of oxy-PAHs for experiments at 1000 and 500 Nm^3 h^{-1} are given in Table 3, together with the corresponding flow, FGR and O$_2$ level and off-gas temperature averages for the given experiments. The total concentration of the measured oxy-PAHs was found to have a 97% and 99% correlation with the average levels of FGR and O$_2$, respectively, for the various experimental

steps. An elevation of the oxy-PAH concentration for experiments at high FGR and high flow is also found here, as for nitro-PAHs.

1,2-Benzanthraquinone is the most abundant of the measured oxy-PAH species in 7 out of 9 samples, making up between 41.2 and 69.1% of the total concentration of the total measured oxy-PAH level, followed by 9,10-anthraquinone, accounting for up to 43.5% of the total amount in some samples. A comparison between the oxy-PAH concentration and

© 2024 The Author(s). Published by the Royal Society of Chemistry

Environ. Sci.: Adv., 2024, **3**, 239–248 | **245**

(a)

(b)
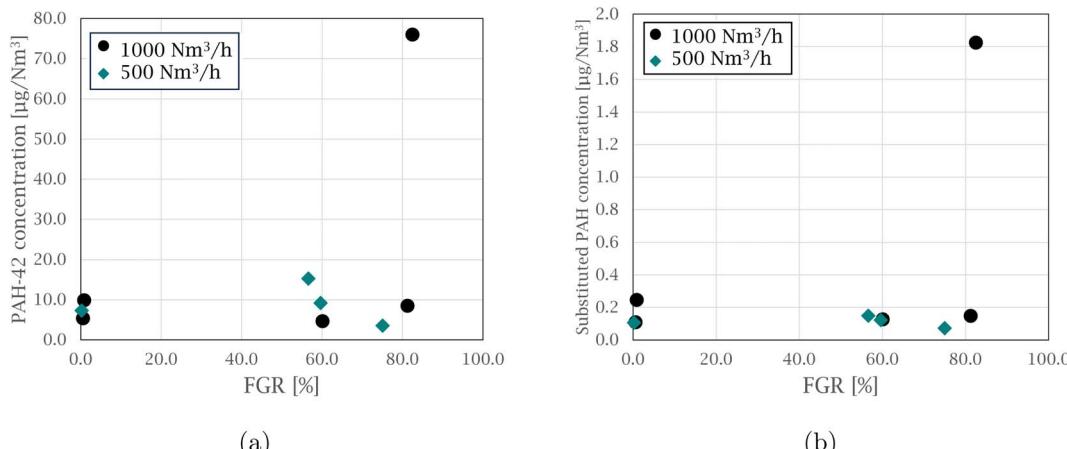
Fig. 6 Graphs showing the estimated PAH stack emissions for PAH-42 and substituted PAHs (sum of oxy- and nitro-PAHs) for both 1000 Nm^3 h^{-1} and 500 Nm^3 h^{-1} at varying FGR levels. (a) PAH-42 and (b) substituted PAH.

their parent PAH is presented in Fig. 5. Fluorene species are shown in Fig. 5(a) and (b), and fluorene is in abundance for all samples but one (the experiment at 59.6% FGR is the exception where the levels are approximately equal). 9,10-Anthraquinone is the dominating species in the anthracene comparison in Fig. 5(c) and (d), but 2-methyl-9,10-anthraquinone is also equal to or exceeds the concentration level of anthracene. Compared to the nitro-PAH species with anthracene as its parent molecule, their oxy-PAH equivalents are in abundance. In Fig. 5(e) and (f), oxy- and nitro-PAH species are compared with their parent PAH, benz[a]anthracene. 7-Nitrobenz[a]anthracene is not produced at significant levels for the experiments at 0% FGR, but increases with increasing FGR, where it exceeds its parent molecule. As with the other quinone molecules already mentioned, 1,2-benz[a]anthraquinone is found in high concentration in all experiments, compared to benz[a]anthracene, especially with increased FGR.

Even though only a small range of substituted PAHs were analyzed and some PAHs are not investigated, such as bicyclic PAHs, a trend is observed. In general, oxy-PAHs follow the same trend as nitro-PAHs and increase at higher levels of FGR. With increasing FGR, the substituted oxy species are equal to or exceed their parent PAH in concentration. These findings are in agreement with the study by Drotikova et al.[19] 9-Fluorenone and 9,10-anthraquinone were found to be the dominating oxy-PAH emissions from a coal power plant in Svalbard. Albinet et al.[33] also found 9,10-anthraquinone to correlate with emission from diesel engines and described the observation as a result of gas-phase formation by ozonation. This coincides with quinones being a result of high temperature combustion processes, as the formation mechanisms that create nitro-PAHs are also applicable to oxy-PAHs. The observation where some diesel particle filters are seen to facilitate the formation of substituted PAHs[16] is interesting in terms of possible parallels to the Si process, where SiO and SiO_2 PM can have a catalytic effect on radical formation or on the formation of PAH precursors and substituted PAHs.

Estimation of PAH stack emissions

An estimation of the PAH emissions from the FGR pilot experiments is presented in Fig. 6. Fig. 6(a) shows the PAH-42 emissions and Fig. 6(b) shows the combined oxy- and nitro-PAH emissions, both at varying FGR levels. The estimation was based on how much of the PAH emissions in each experimental cycle passed through the glass fiber filter used in the sampling set-up and the amount of process gas not being recycled back to the furnace, but exited the stack.

Even though process and temperature variations were not taken into account, an indication towards the PAH emissions, both PAH-42 and substituted PAHs, not being significantly increasing with added FGR is shown, as more of the increased PAHs produced would be recirculated back to the furnace. The exception is the case at 1000 Nm^3 h^{-1} and 82.5% FGR in both Fig. 6(a) and (b), where the filter efficiency is lower due increasing the production of PAHs of low molecular weight, which can pass through the filter.[30] This experiment measured on average 13.3 vol% oxygen in the furnace atmosphere and together with the general decreased off-gas temperature and residence time for the PAHs at the 1000 Nm^3 h^{-1} flow rate, and these furnace conditions could provide poor overall combustion conditions for PAH degradation.

Conclusions

In this study, the substituted PAH emissions of oxy- and nitro-PAHs, with a size of 3 to 5 rings, were measured from a silicon process. A measurement campaign was performed where a Si alloy was produced continuously in a pilot scale submerged arc furnace with FGR and various levels of O_2 and flue gas flow to investigate how FGR influenced furnace operation and off-gas composition. Isokinetic sampling in the off-gas duct was performed to measure PAH levels under varying conditions and analyzed using GC-qToF. The concentration levels for oxy-PAHs were in the range of 1.1 to 4.4 μg Nm^{-3}, without FGR, and increased to 36.6 μg Nm^{-3}, at 82.5% FGR. For

nitro-PAHs, the concentration range was between 1.4 and 1.9 µg Nm^{-3}, without FGR, and increased to 65.9 µg Nm^{-3}, at 81.3% FGR. With FGR, substituted PAH species, such as 4-nitropyrene and 1,2-benzanthraquinone, were produced in greater amounts than their parent PAHs. Even though the concentration of PAHs measured in the off-gas duct increases with FGR, no significant change is found in the stack emissions with estimations based on the amount of PAHs passing through the filter used for sampling, except for PAHs of low molecular weight. Comparing the two flue gas flows, experiments at 500 Nm^3 h^{-1} produced overall lower amounts of substituted PAHs, as well as less SiO_2 PM and NO_x, as caused by less oxygen available for combustion, increased temperature in the off-gas and increased residence time in the combustion zone.

Conflicts of interest

There are no conflicts to declare.

Acknowledgements

References

1 H. I. Abdel-Shafy and M. S. M. Mansour, A review on polycyclic aromatic hydrocarbons: source, environmental impact, effect on human health and remediation, *Egypt. J. Pet.*, 2016, **25**, 107–123.

2 M. Howsam and K. C. Jones, PAHs and Related Compounds: Chemistry, in *The Handbook of Environmental Chemistry*, ed. A. H. Neilson, Springer Berlin Heidelberg, Berlin, Heidelberg, 1998, pp. 137–174.

3 A. Schei, J. Tuset and H. Tveit, *Production of High Silicon Alloys*, Tapir, Trondheim, 1998.

4 N. E. Kamfjord, Mass and energy balances of the silicon process: improved emission standards, *PhD thesis*, Norwegian University of Science and Technology, Trondheim, 2012.

5 I. Kero, S. Grådahl and G. Tranell, Airborne Emissions from Si/FeSi Production, *JOM*, 2017, **69**, 365–380.

6 H. Gaertner, T. A. Aarhaug, B. Wittgens, L. Hunsbedt, M. Legård and G. Tranell, *The 15th International Ferroalloys Congress INFACON XV*, Southern African Institute of Mining and Metallurgy, Cape Town, 2018.

7 S. Thomas and M. J. Wornat, The effects of oxygen on the yields of polycyclic aromatic hydrocarbons formed during the pyrolysis and fuel-rich oxidation of catechol, *Fuel*, 2008, **87**, 768–781.

8 A. I. H. Hrdina, I. N. Kohale, S. Kaushal, J. Kelly, N. E. Selin, B. P. Engelward and J. H. Kroll, The Parallel Transformations of Polycyclic Aromatic Hydrocarbons in the Body and in the Atmosphere, *Environ. Health Perspect.*, 2022, **130**(2), 25004.

9 B. A. M. Bandowe and H. Meusel, Nitrated polycyclic aromatic hydrocarbons (nitro-PAHs) in the environment – a review, *Sci. Total Environ.*, 2017, **581–582**, 237–257.

10 World Health Organization, *Agents Classified by the IARC Monographs, Volumes 1–132 – IARC Monographs on the Identification of Carcinogenic Hazards to Humans*, 2022, https://monographs.iarc.who.int/agents-classified-by-the-iarc/.

11 A. R. Katritzky, M. S. Kim, D. Fedoseyenko, K. Widyan, M. Siskin and M. Francisco, The sulfonation of aromatic and heteroaromatic polycyclic compounds, *Tetrahedron*, 2009, **65**(20), 4709–4872.

12 A. Albinet, E. Leoz-Garziandia, H. Budzinski, E. Villenave and J. L. Jaffrezo, Nitrated and oxygenated derivatives of polycyclic aromatic hydrocarbons in the ambient air of two French alpine valleys: Part 1: Concentrations, sources and gas/particle partitioning, *Atmos. Environ.*, 2008, **42**, 43–54.

13 M. Carrara, J.-C. Wolf and R. Niessner, Nitro-PAH formation studied by interacting artificially PAH-coated soot aerosol with NO2 in the temperature range of 295–523K, *Atmos. Environ.*, 2010, **44**, 3878–3885.

14 R. Atkinson, E. C. Tuazon and J. Arey, Reactions of naphthalene in N2O5-NO3-NO2- air mixtures, *Int. J. Chem. Kinet.*, 1990, **22**, 1071–1082.

15 I. J. Keyte, R. M. Harrison and G. Lammel, Chemical reactivity and long-range transport potential of polycyclic aromatic hydrocarbons – a review, *Chem. Soc. Rev.*, 2013, **42**, 9333–9391.

16 N. V. Heeb, *et al.*, Secondary Effects of Catalytic Diesel Particulate Filters: Conversion of PAHs versus Formation of Nitro-PAHs, *Environ. Sci. Technol.*, 2008, **42**, 3773–3779.

17 K. Hayakawa, Environmental Behaviors and Toxicities of Polycyclic Aromatic Hydrocarbons and Nitropolycyclic Aromatic Hydrocarbons, *Chem. Pharm. Bull.*, 2016, **64**, 83–94.

18 C. Walgraeve, K. Demeestere, J. Dewulf, R. Zimmermann and H. Van Langenhove, Oxygenated polycyclic aromatic hydrocarbons in atmospheric particulate matter: Molecular characterization and occurrence, *Atmos. Environ.*, 2010, **44**, 1831–1846.

19 T. Drotikova, A. M. Ali, A. K. Halse, H. C. Reinardy and R. Kallenborn, Polycyclic aromatic hydrocarbons (PAHs) and oxy- and nitro-PAHs in ambient air of the Arctic town Longyearbyen, Svalbard, *Atmos. Chem. Phys.*, 2020, **20**, 9997–10014.

20 F. Normann, R. Skafestad, M. Bierman, J. Wolf and A. Mathisen, *Reducing the Cost of Carbon Capture in Process Industry*, 2019, https://www.sintef.no.

21 A. Mathisen, F. Normann, M. Biermann, R. Skagestad and A. T. Haug, *CO2 Capture Opportunities in the Norwegian Silicon Industry*, SINTEF Academic Press, 2019.

22 E. Sher, *Handbook of Air Pollution from Internal Combustion Engines*, ed. E. Sher, Academic Press, San Diego, 1998, pp. 27–41.

23 S. Chen, K. Cui, J. Zhu, Y. Zhao, L.-C. Wang and J. K. Mutuku, Effect of Exhaust Gas Recirculation Rate on the Emissions of Persistent Organic Pollutants from a Diesel Engine, *Aerosol Air Qual. Res.*, 2019, **19**, 812–819.

© 2024 The Author(s). Published by the Royal Society of Chemistry

Environ. Sci.: Adv., 2024, **3**, 239–248 | **247**

24 M. Abdelaal, M. El-Riedy and A. El-Nahas, Effect of flue gas recirculation on burner performance and emissions, *Journal of Al-Azhar University Engineering Sector*, 2016, **11**(41), 1275–1284.

25 P. Liu, Y. Zhang, L. Wang, B. Tian, B. Guan, D. Han, Z. Huang and H. Lin, Chemical Mechanism of Exhaust Gas Recirculation on Polycyclic Aromatic Hydrocarbons Formation Based on Laser-Induced Fluorescence Measurement, *Energy Fuels*, 2018, **32**, 7112–7124.

26 B. Wittgens, B. Panjwani, T. Pettersen, R. Jensen, B. Ravary and D.-O. Hjernes, SCORE: Staged Combustion for Energy Recovery in Ferro-alloy Industries – Experimental Validation, *Infacon XV: International Ferro-Alloy Congress*, Southern African Institute of Mining and Metallurgy, Cape Town, 15th edn, 2018.

27 V. Andersen, Flue Gas Recirculation for the Silicon Process, *PhD thesis*, Norwegian University of Science and Technology, Trondheim, 2023.

28 V. Andersen, I. Solheim, H. Gaertner, B. Sægrov-Sorte, K. E. Einarsrud and G. Tranell, Pilot-Scale Test of Flue Gas Recirculation for The Silicon Process, *J. Sustain. Metall.*, 2022, **9**, 81–92.

29 V. Andersen, I. Solheim, H. Gaertner, B. Sægrov-Sorte, K. E. Einarsrud and G. Tranell, in *REWAS 2022: Developing Tomorrow's Technical Cycles (Volume I)*, ed. A. Lazou, K. Daehn, C. Fleuriault, M. Gökelma, E. Olivetti and C. Meskers, Springer International Publishing, Cham, 2022, pp. 555–564.

30 K. Arnesen, K. J. Vachaparambil, V. Andersen, B. Panjwani, K. Jakovljevic, E. K. Enge, H. Gaertner, T. A. Aarhaug, K. E. Einarsrud and G. Tranell, Analysis of Polycyclic Aromatic Hydrocarbon Emissions from a Pilot Scale Silicon Process with Flue Gas Recirculation, *Ind. Eng. Chem. Res.*, 2023, **62**(19), 7525–7538.

31 National Institute of Health, *PubChem*, 2022, **https://pubchem.ncbi.nlm.nih.gov/**.

32 S. Hu, J. D. Herner, W. Robertson, R. Kobayashi, M.-C. O. Chang, S.-m. Huang, B. Zielinska, N. Kado, J. F. Collins, P. Rieger, T. Huai and A. Ayala, Emissions of polycyclic aromatic hydrocarbons (PAHs) and nitro-PAHs from heavy-duty diesel vehicles with DPF and SCR, *J. Air Waste Manage. Assoc.*, 2013, **63**, 984–996.

33 A. Albinet, E. Leoz-Garziandia, H. Budzinski and E. ViIlenave, Polycyclic aromatic hydrocarbons (PAHs), nitrated PAHs and oxygenated PAHs in ambient air of the Marseilles area (South of France): Concentrations and sources, *Sci. Total Environ.*, 2007, **384**, 280–292.